Tellus
SERIES A
DYNAMIC
METEOROLOGY
AND OCEANOGRAPHY
PUBLISHED BY THE INTERNATIONAL METEOROLOGICAL INSTITUTE IN STOCKHOLM

Tellus (2011), 63A, 158–173
Printed in Singapore. All rights reserved

TELLUS

Future climate impact on spruce bark beetle life cycle in relation to uncertainties in regional climate model data ensembles

By ANNA MARIA JÖNSSON[1]* and LARS BÄRRING[2], [1]*Division of Physical Geography and Ecosystem Analysis, Department of Earth and Ecosystem Sciences, Lund University, Sölvegatan 12, SE-223 62 Lund, Sweden;* [2]*Rossby Centre, Swedish Meteorological and Hydrological Institute, SE-601 76, Norrköping, Sweden*

(Manuscript received 2 February 2010; in final form 17 August 2010)

ABSTRACT

In this study, we quantify the effect of uncertainties in climate projections on an impact model (IPS) that describes the temperature-dependent swarming and development of *Ips typographus*. Three forcing climate data sets (ensembles) were used: (1) E-Obs gridded observations, (2) ERA-40 reanalysis data downscaled by eight regional climate models (RCMs) and (3) regional scenarios from one RCM forced by seven GCM simulations representing SRES-A1B, for the period of 1961–2097. The *IPS_RCM_ERA40* ensemble members, including *IPS_RC3_ERA40*, were generally within the *IPS_E-Obs* confidence limits. The IPS model is however sensitive to the warming during spring and cooling during autumn, and deviations in simulated swarming were related to known climate model biases. The variation between the *IPS_RCA3_GCM* ensemble members was particularly high in regions where warmer summers (temperature increase from +2 °C to +4 °C) will induce an additional generation per year, for example a shift from one to two generations per year in south Scandinavia, and an increased frequency of three generations per year in central Europe. Impact assessments based on an ensemble of climate data gives more robust decision support than a single climate model approach because it allows a probabilistic assessment of the geographical areas experiencing a transition in biological response.

1. Introduction

1.1. Climate model data ensembles

The use of regional climate models (RCMs) for dynamical downscaling of global climate scenarios, produced by general circulation models (GCMs), is often a necessary step for enabling analyses of climate change impacts. The higher spatial resolution allows RCMs to better represent climate extremes and spatial variations in regional climate (Kjellström et al., 2007; Nikulin et al., 2011), and by design they maintain the physical consistency among the variables produced by the GCMs (Rummukainen, 2010). With recent efforts to coordinate regional downscaling activities over Europe, comprehensive databases of RCM output now exist. In the ENSEMBLES project (van der Linden & Mitchell, 2009), the downscaling performance of an ensemble of RCMs was evaluated in a consistent and coordinated way (Christensen et al., 2009), by using the ERA40 reanalysis data set based on weather observations (Uppala et al., 2005) as lateral boundary conditions for the period 1961–1990. Another undertaking of the ENSEMBLES project was to use the RCMs to create an ensemble of regional climate scenarios by forcing different RCMs with data from different GCMs as lateral boundary conditions. The design matrix (GCM × RCM) is however not complete, and in some sense sparse. Kjellström et al. (2011) therefore used the Rossby Centre RCM RCA3 (Kjellström et al., 2005; Samuelsson et al., 2011) to downscale a comparatively large set of GCM output. An advantage with this ensemble is that the same RCM is used to produce all downscaled scenarios. This limits the information regarding the performance of different RCMs in future climates but makes it easier to disentangle other aspects of the uncertainty, in particular what is introduced by different GCM model formulations, and initial conditions.

In this study, we take the approach of ensemble-based analysis of climate change projections one step further by addressing the chain GCM–RCM–ecological impact model. The strategy is to assess the impact model uncertainty by using the RCM_ERA40 ensemble, of which RCA3 is one ensemble member, in combination with the A1B scenario ensemble produced by RCA3.

*Corresponding author.
e-mail: Anna_Maria.Jonsson@nateko.lu.se
DOI: 10.1111/j.1600-0870.2010.00479.x

1.2. Ecosystem impacts of climate change

Changes in timing of spring phenology, life cycle events and geographical distribution of plants and animals, among them several insect species, have been related to the changes in climate that have occurred during the last decades (Walther et al., 2002; Parmesan, 2006). The increasing focus on climate change impacts on natural and managed ecosystems (Rosenzweig et al., 2007) includes both concerns about species conservation (Araujo and Rahbek, 2006) and insect outbreaks (Ayres and Lombardero, 2000). This has created a need for impact modelling that can frame these concerns and convert the state-of-the art climate scenarios into information about vegetation dynamics and specific response of different key species.

Phenological modelling is a useful tool for simulating temperature impact on the life cycle of insects. Quantitative assessments of biological responses to climate change commonly include both response thresholds and cumulative effects, for example the developmental process from egg to mature insect is typically controlled by both temperature thresholds and temperature sums (Annila, 1969; Wermelinger and Seifert, 1998; Gray, 2004). The impact assessment therefore crucially depends on the climate scenario data that are used for driving biological impact models. As with climate change analyses in general, uncertainties associated with climate modelling have to be considered when interpreting the results of biological impact modelling (Déqué et al., 2007; Olesen et al., 2007).

1.3. Impact of spruce bark beetles (*Ips typographus*)

Extreme weather events such as windstorms, dry spells and flooding are driving factors in forest disturbance dynamics (Oliver and Larson, 1996; Franklin et al., 2002; Hanewinkel et al., 2008). Insects and pathogens may utilize trees killed or weakened by disturbances as breeding material and several herbivorous insect species, bark beetles in particular, have the potential to aggravate the damage caused by disturbances (Schelhaas et al., 2003; Rouault et al., 2006; Fettig et al., 2007). The spruce bark beetle (*I. typographus* L. Coleoptera, Scolytidae) can attack mature and economically important stands of Norway spruce (*Picea abies*). Norway spruce, one of the dominating tree species in Northern and Central Europe, is highly vulnerable to windthrow (Nilsson et al., 2004; Nilsson, 2008). A secondary consequence of recent severe windstorms is that millions of standing spruce trees were killed in large-scale bark beetle outbreaks. Such large outbreaks can develop when there is a large volume of wind thrown trees that provide ample breeding material supporting a large increase in population size (Christiansen and Bakke, 1988; Schelhaas et al., 2003; Økland and Berryman, 2004; Økland and Bjørnstad, 2006). Tree mortality generally peaks a few years after the storm disturbance (Schroeder, 2003), although summer drought reducing host tree resistance can result in prolonged mortality periods (Økland and Bjørnstad, 2003; Rouault et al., 2006; Faccoli, 2009). To sustain a bark beetle population, the climate of a region must at least allow one generation to complete its development in 1 year as the winter mortality of immature stages is very high (Faccoli, 2002).

Climate change is expected to influence the damaging potential of *I. typographus* via effects on tree defence capacity and temperature influence on insect flight activity and developmental rate, leading to a gradually increased frequency of an additional generation per year (Lange et al., 2006; Jönsson et al., 2007). In south Scandinavia, *I. typographus* may thus shift from primarily producing one generation to regularly producing two generations per year (Jönsson et al., 2009). Due to the potentially serious consequences for forest protection and production economy there is need for analysing the consequences of projected climate change to support the development of adaptation strategies, including forest management actions (Seidl et al., 2009).

1.4. Effect of uncertainties in climate projections on impact model performance

Previous studies of climate change impact on the number of *I. typographus* generations per year (voltinism) have used driving data from a combination of one regional and one global climate model (Lange et al., 2006; Jönsson et al., 2007), and extending the analyses to several emission scenarios (Jönsson et al., 2009). The climate data sets used in earlier studies did however not allow any assessment of the sensitivity of the impact model to variations in dynamical downscaling or lateral forcing of the RCM. In this study we will make use of two newly produced climate data ensembles (Christensen et al., 2009; Kjellström et al., 2011) for extending previous studies by analysing how the bark beetle model (Jönsson et al., 2007) responds to uncertainties inherent in the regional and global climate simulations. As reference we use a gridded observational data set that is independent of RCM downscaled data. In this way we are able to carry out an initial probabilistic assessment of climate change impact on voltinism of *I. typographus*.

2. Material and Methods

2.1. IPS model

In this study we used the model developed by Jönsson et al., (2007), hereafter denoted the IPS model, to analyse the climate change impact on bark beetle activity. Model calculations were based on a daily timestep. A maximum temperature, *T2max*, threshold controls reproductive flight activity, and accumulation of daily mean temperature, *T2mean*, controls the timing of completed maturation of the new generation (Fig. 1). Thermal sums were expressed as degree-days (dd) above a developmental threshold, which was set to $+5\ ^{\circ}$C for all stages according to (Annila, 1969). The emergence of the parental generation

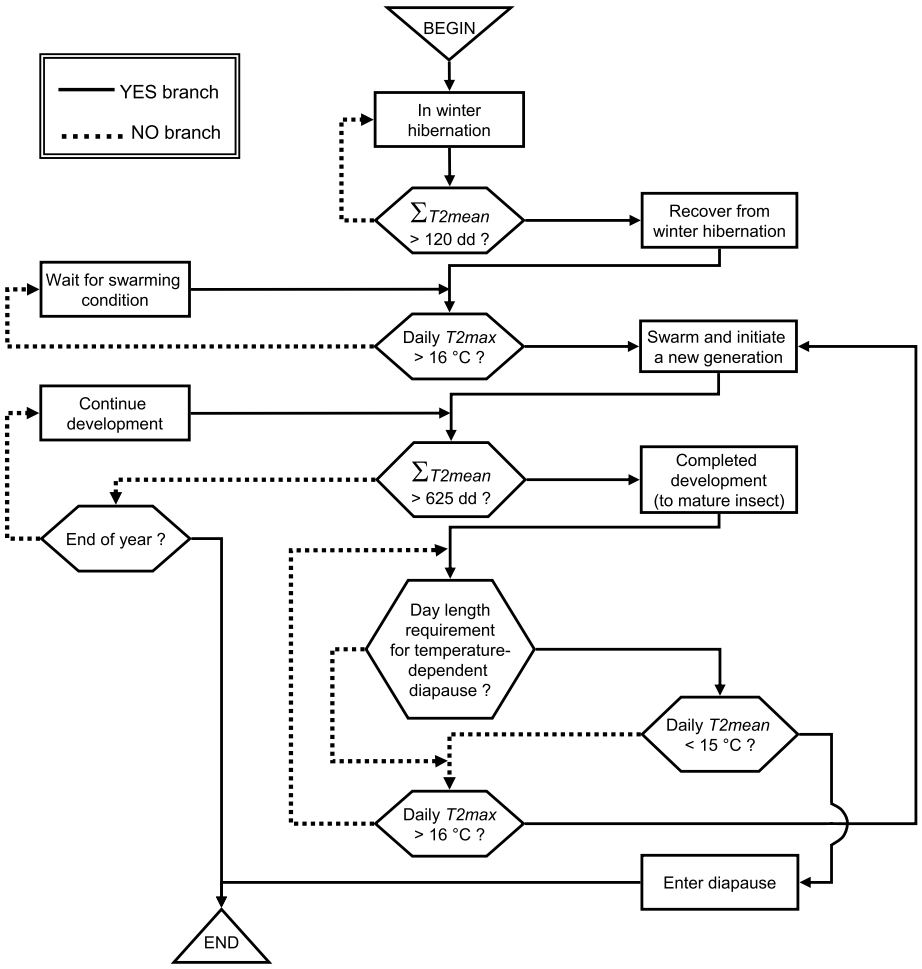

Fig. 1. The logical structure of the temperature-dependent calculation steps included in the bark beetle model. The IPS model simulates the phenological stages of bark beetle development for each year. The annual simulation begins with the bark beetle population being in winter hibernation. The model is then stepped forward in daily time-steps until the end of the year or when diapause conditions are reached.

after winter hibernation was set to 120 dd (Annila, 1969). Flight activity was set to occur when the daily maximum temperature exceeded 16 °C, based on temperature threshold calibration and validation using pheromone trap monitoring data (Jönsson et al., 2009, 2010). Egg development was modelled to start 7 days later, accounting for a pre-oviposition period with mating (Wermelinger and Seifert, 1999), and time to lay half of the egg clutch (Anderbrant, 1990). In this study, the developmental time from egg to mature bark beetle was calculated for development in sun-exposed brood trees, corresponding to 625 dd (Jönsson et al., 2007), as this is preferred over shaded conditions by *I. typographus* (Christiansen and Bakke, 1988). The model calculations account for up to three generations per year.

Reproductive diapause is the adaptive response to cues from day length and temperature to avoid unsuccessful reproduction at a time when a new generation is unlikely to reach maturity before winter (Dolezal and Sehnal, 2007). Diapause reduces the probability that a large proportion of the population will not be able to survive winter due to incomplete development, although this may still occur during cold autumns. Without reproductive diapause, however, initiations of a second and a third generation would have been much more common than observed. Model representation of reproductive diapause is therefore required. The reproductive diapause was modelled to occur after fulfilment of a day length requirement and subsequent temperature requirement, $T2mean < 15$ °C, when day length is shorter than a local threshold value (Jönsson et al., 2010). The day length setting corresponds to the natural selection during years with cold autumn temperatures. The gridcell-specific threshold was parameterized as the day length of the earliest date during a 30-year period when the bark beetles were not able to reach the maturity state required for surviving winter. This parameterization, which has been evaluated against independent field monitoring data (Jönsson et al., 2010), approximately follows a latitudinal gradient from 15–16 h in the south of the study area to 20–22 h in the north.

The day length requirements of insect species may rapidly adjust to changes in climate (van Asch et al., 2007). In this study, the parameterization was based on the assumption that *I. typographus* has the potential for fast adaptation to new climate conditions by migration and natural selection. The local day length threshold was therefore recalculated for each 30-year period. This implies an increase in length of summer flight periods by up to 1 week by the end of this century in comparison to simulations where adaptation is not accounted for (Jönsson et al., 2010). Fig. 2 illustrates the different modelling steps for one grid cell, including the interannual variation, during the first and last simulated 30-year periods.

2.2. Climate data sets

Three different climate data sets covering Europe were used in this study, all having a spatial resolution of approximately 50 × 50 km: (1) The *E-Obs* gridded European weather data set covering the period 1961–1990 (Haylock et al., 2008) available through the URL http://eca.knmi.nl/ensembles. This data set is based on a large number of daily observations from a network of meteorological stations. For each day the available observations were gridded by means of statistical interpolation techniques to produce both a best estimate and an upper and lower 95% confidence bound for each gridcell and day. Consequently, this data set provides information on the uncertainty range inherent in observations of the climatic conditions. It was used for evaluation purposes, as it is fully independent of climate models. (2) An ensemble of data from eight different RCMs (Christensen et al., 2009; Table 1) forced by the ERA40 reanalysis data (Uppala et al., 2005) for the period 1961–1990. This data set, herein denoted as *RCM_ERA40*, was developed within the ENSEMBLES project (van der Linden & Mitchell, 2009) and is available through the ENSEMBLES data archive (URL: http://ensemblesrt3.dmi.dk). RCA3 (Kjellström et al., 2005; Samuelsson et al., 2011) is one of the RCMs in this ensemble, and this specific run is denoted *RCA3_ERA40* in the following. (3) Out of an ensemble of 16 regional climate scenarios experiments produced by RCA3 (Kjellström et al., 2011) seven runs were selected for this study. All selected runs represent the SRES A1B climate change scenario (Nakićenović and Swart, 2000) for the period of 1961–2097. Lateral boundaries were taken from seven different GCM formulations (Table 1). There are five different GCMs of which one, HadCM3, were run with three different climate sensitivity settings (Collins et al., 2010). For the purpose of this paper, this ensemble is denoted *RCA3_GCM*.

In our analyses, the scenarios were divided into three periods: 1961–1990, 2011–2040 and 2070–2097. The latter period only comprise 28 years because for some model runs data were not available up to including year 2100. The summer mean temperature change of individual ensemble members ranges from 2 to 4 °C (Kjellström et al., 2011). In the study area *RCA3_HadCM3ref* shows the strongest warming signal (about 3–4 °C) and *RCA3_BCM* exhibits a more modest warming of about 2–3 °C over of the whole study area. The other ensemble members show trends that fall in between these two runs, and the general pattern of warming in the study region is broadly similar: strongest warming in the south (Mediterranean) and east (continental), as well as in the far north (Arctic). And the Baltic Sea region (air temperature) is projected to warm more than the surrounding land areas.

2.3. Overview of the IPS simulation and evaluation strategy

The IPS model was run for all data series/ensemble members listed in Table 1, thus generating output for (i) the *IPS E-Obs* data set (three series), (ii) the *IPS RCM_ERA40* ensemble (eight series) and (iii) the *IPS RCA3_GCM* ensemble (seven series). The reference period 1961–1990 is common to all data series. The data sets were evaluated in four steps: First, we analyse how the observational uncertainty (quantified by the *E-Obs* lower and upper 95% confidence limits) is carried over to the IPS model output, and how this uncertainty compares to the variation in the *IPS RCM_ERA40* ensemble, which represents the downscaling uncertainty. Secondly, by comparing the *IPS RCA3_ERA40* run with the other members of the *IPS RCM_ERA40* ensemble, we establish a basis for putting the *IPS RCA3_GCM* climate change simulations into the context of uncertainties related to the different RCMs. Thirdly, for the *IPS RCA3_GCM* ensemble we follow the standard procedure of using the *RCA3_ERA40* run as the reference climate data set. Thus, the *RCA3-ERA40* run is used for linking the two ensembles in the reference period 1961–1990. Finally, to assess the projected climate change impact the three periods available in the *IPS RCA3_GCM* ensemble were compared.

We focus our analyses on the timing of four key events: (a) day number when the first generation of *I. typographus* is initiated, that is date when the blue lines of Fig. 2 begin, (b) day number when the development of the first generation is completed (blue lines end), (c) day number when the second generation is initiated (green lines begin) and, finally, (d) day number when the third generation is initiated (red lines begin). In this study, we assessed climate impact on the initiation of a second and a third generation. The population dynamics during outbreaks, with a potentially large population growth from one generation to the next, implies that both these generations can kill standing trees regardless of whether the new generation will reach maturity or not. The completed development from egg to mature bark beetle is, however, of importance for survival during the winter season, and thus the potential damage during the next year. However, the reproductive success, and the population dynamics from 1 year to the next, is not yet included in the model.

The entire study area was selected to cover the main distribution area of *Picea abies*, which includes several bioclimatic

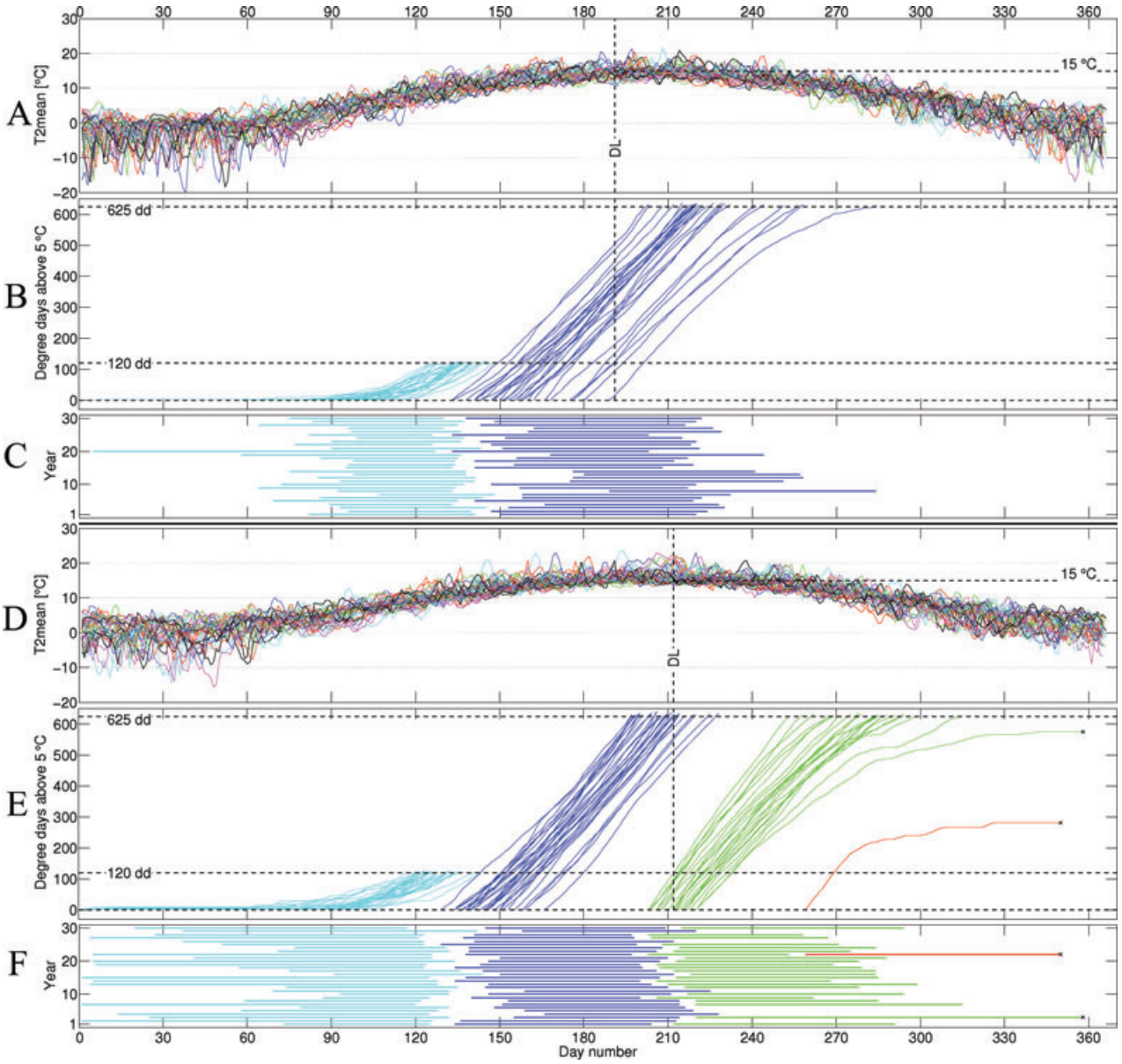

Fig. 2. Interannual variation in the different IPS modelling steps for a typical gridcell in southern Sweden (57°N 14.7°E). Panels A–C show the result of using climate forcing from *RCA3_ECHAM5_A1B* reference period (1961–1990), and panels D–F show the corresponding results for the future scenario period 2070–2097. Panels A and D show the annual cycle of daily mean temperature (*T2mean*) for the individual years. Panels B and E show the accumulation of degree-days for the different simulation steps. Cyan: accumulation up to 120 dd, accounting for the recovery of the parental generation from winter hibernation. Blue: reproductive flight initiates the development of the first generation, which reaches maturation at 625 dd. The future warmer climate (panel E) allows a second generation (green) to reach maturity in 23 out of the 29 years. For 1 year, the temperature did not allow completed development of the second generation, which is marked by a black cross. For another future year, the temperature allowed for initiation of a third generation (red), although it did not reach maturity. The dashed lines marked 'DL' refers the timing when initial cues from day length may initiate diapause if *T2mean* drops below the 15 °C threshold (see Section 2.1 for details). Panels C and F show for each year (horizontal) the duration of each successive step and the varying time between completed development and swarming conditions.

zones (Ahti et al., 1968). Six regions were selected to provide detailed analysis of the variability within and between the different IPS model runs (Fig. 3). Region 1 (40 gridcells) represents the sub-artic and boreo-montane biotic zone of northernmost Sweden and Finland. Region 2 (43 gridcells) represents the boreal zone of southern Finland. The boreo-nemoral zone is covered by region 3 (42 gridcells in Sweden) and region 4 (42 gridcells in the Baltic states and Belarus). The nemoral zone of

Table 1. List of the gridded climate time-series, that is ensemble members, included in the three data sets used in this study: (1) *E-Obs*, (2) the *RCM_ERA40* ensemble and (3) the *RCA3_GCM* ensemble, where the shorthand model name used in the text is underlined.

E-Obs (Haylock et al., 2008)	*RCM_ERA40* ensemble	*RCA3_GCM* ensemble (Kjellström et al., 2011; Nikulin et al., 2011)
Lower 95% confidence bound	DMI-HIRHAM (Christensen et al., 1996)	HADCM3-Q0 (ref) (Gordon et al., 2000)
Best estimate	ETHZ-CLM (Böhm et al., 2006)	HADCM3-Q16 (high) (Gordon et al., 2000)
Upper 95% confidence bound	RACMO2 (van Meijgaard et al., 2008)	HADCM3-Q3 (low) (Gordon et al., 2000)
	METNO-HIRHAM (Christensen et al., 1996; Haugen and Haakenstad, 2006)	ECHAM5/MPI-OM (Jungclaus et al., 2006; Roeckner et al., 2006)
	HadRM3.0 (Buonomo et al., 2007)	BCCR-BCM2.0 (Bleck et al., 1992; Déqué et al., 1994)
	REMO (Jacob, 2001; Jacob et al., 2001)	CCSM3 (Collins et al., 2006)
	RCA3 (Kjellström et al., 2005; Samuelsson et al., 2011)	CNRM-CM3 (Déqué et al., 1994; Royer et al., 2002)
	GKSS-CLM (Böhm et al., 2006)	

Note: All data sets use the same spatial resolution and grid specifications.

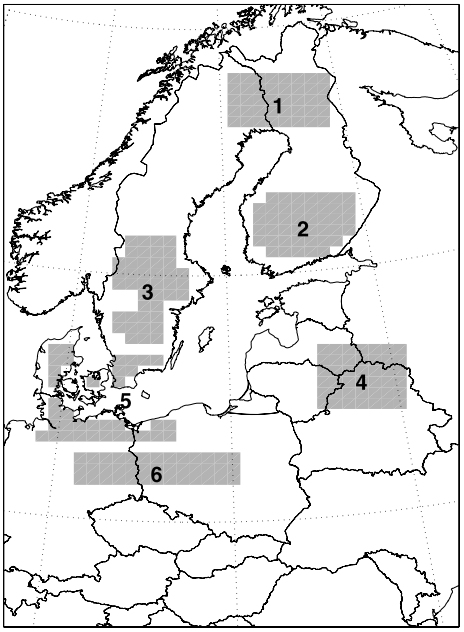

Fig. 3. Map of the six regions discussed in the text and shown in Figs 4 and 5. The regions are selected to cover different aspects of climate change impacts in bark beetle voltinism. Region 5 comprises the land areas surrounding the SW Baltic and the Danish Straits.

Denmark, northern Germany and Poland is represented by region 5 (36 gridcells) and region 6 (39 gridcells), having a costal climate and a continental climate, respectively. The regions covers different aspects of climate change impacts on bark beetle activity, representing areas changing from zero to one generation per year (region 1), from one to two (region 2 and 3) and from two to three generations per year (regions 4–6). The regions were selected so that the gridcells had reasonably homogeneous IPS modelling results. This enabled us to focus on the gradual increase of an additional generation per year, and reduce the effect of small-scale variability (spatial noise) that can be pronounced in a single-gridcell analysis. In particular, we did not carry out any detailed regional analysis in mountainous regions, as the altitudinal impact on climate would have created a mixed signal.

The impact of climate variability within the *IPS RCA3_GCM* ensemble was further analysed by calculating percentiles for timing of completed development on the full data set (all years in each period, and all gridcells in each region). For each gridcell, years when the last produced generation was calculated to not reach maturity were assigned an artificially high day number (i.e. above 365). This gives percentiles that are directly comparable in temporal profiles and across regions and models, producing a truncated cumulative frequency distribution where missing percentiles represents missing data.

To capture the large-scale geographical pattern of *I. typographus* voltinism across the whole study area, timing and frequency of bark beetle activity were calculated for the *IPS RCA3_GCM* ensemble for the climate periods of 1961–1990, 2011–2040 and 2070–2097. Standard deviation was used as a measure of variability between *RCA3_GCM* members.

3. Results

3.1. Variability and uncertainty during the reference period 1961–1990

Figure 4 provides an overview of the climate-induced variability in initiation and completion of the first generation of *I. typographus* within all the IPS model runs for the reference period. For both development stages there is a substantial range in timing (as indicated by the plotted 'whiskers') between the coldest data value (late timing) and the warmest observation (early timing). However, for the middle 50% of the data (i.e. data falling between the 25th and 75th percentile, as indicated by the 'boxes') the variability is substantially reduced, typically in the range 10–20 days. The averages of the three data sets (*IPS E-Obs*, the

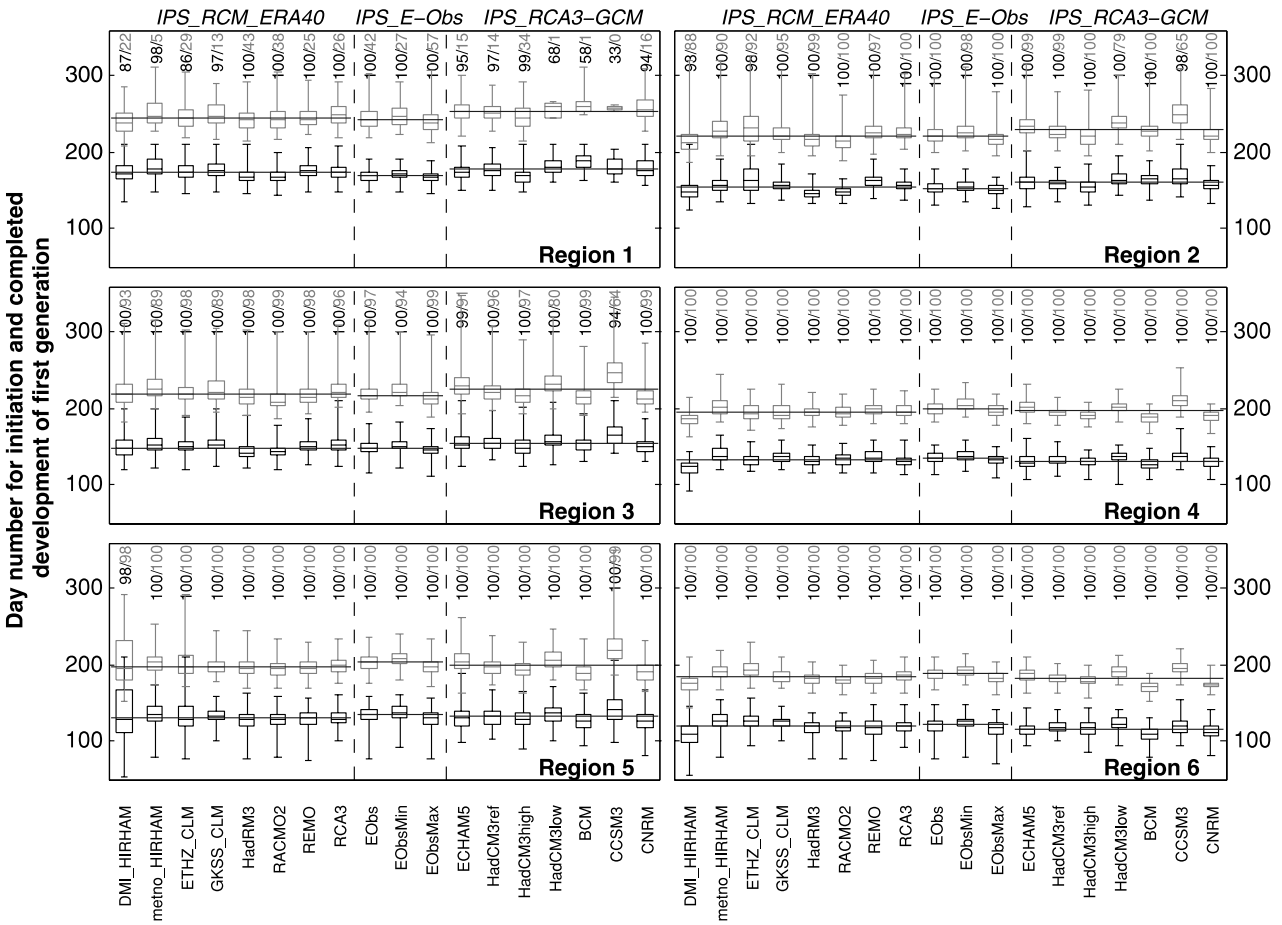

Fig. 4. Comparison of the basic statistics of flight (black boxplots) and completed development (grey boxplots) of the first generation, produced by driving the IPS model with the three different temperature data sets for the reference period 1961–1990 (Table 1): (i) Eight *RCM_ERA40* ensemble members. (ii) *E-Obs* best estimate and the lower and upper 95% confidence limits. (iii) Seven *RCA3_GCM* ensemble members. Data was analysed for the six regions, defined in Fig. 3. The boxplots show the timing of flight and completed development with the median, upper and lower quartile for the different time periods. The whiskers extend to the minimum/maximum values. Data for all gridcells in a region ($n = 36$–43) and all years in the period ($m = 30$) are lumped together, which means that each boxplot is based on more than 1000 data values. The percentage of years when flight (black numbers) and completed development (grey numbers) occurs is indicated above the boxes. The horizontal lines denote the average for each data set.

IPS RCM_ERA40 ensemble and the *IPS RCA3_GCM* ensemble) are relatively close in all regions, whereas the individual ensemble members display a considerable variation.

However, it is not only the variability in timing, as depicted by the boxplots that is of interest, but also how often this stage is reached. The frequency of initiation and completion of the first generation are shown as percentages at the top of each panel of Fig. 4. A local population of *I. typographus* can exist in all regions with the exception of the northernmost region 1. In this region, the calculated frequency of years warm enough to allow for completed development one bark beetle generation differs largely between IPS model runs: The *IPS E-Obs* data set varies between 27% and 57%, the *IPS RCM_ERA40* ensemble between 13% and 43%, and the *IPS RCA3_RCM* between ∼0% and 34%. The low frequency of completed development of the first generation results in decreased span between the earliest and latest timing due to smaller sample size. In particular, for some of the *IPS RCA3_GCM* ensemble members the span is very narrow.

Fig. 5 shows similar boxplots for the initiation of the second and third generations. The climatic limitation of bark beetle development, and thus the variation between IPS model runs, becomes more obvious as the second (third) generation is only initiated if the first (second) generation reaches maturity and initiates a new generation before reproductive diapause. The frequency of more than one generation per year decreases towards the north. A second generation is frequently initiated in regions 4–6, rarely in regions 2 and 3. A third generation sometimes follows in region 6, seldom in regions 4 and 5, and is not seen in regions 1–3.

The regional frequency of occurrence and mean timing of the four key events according to the two RCM ensembles and

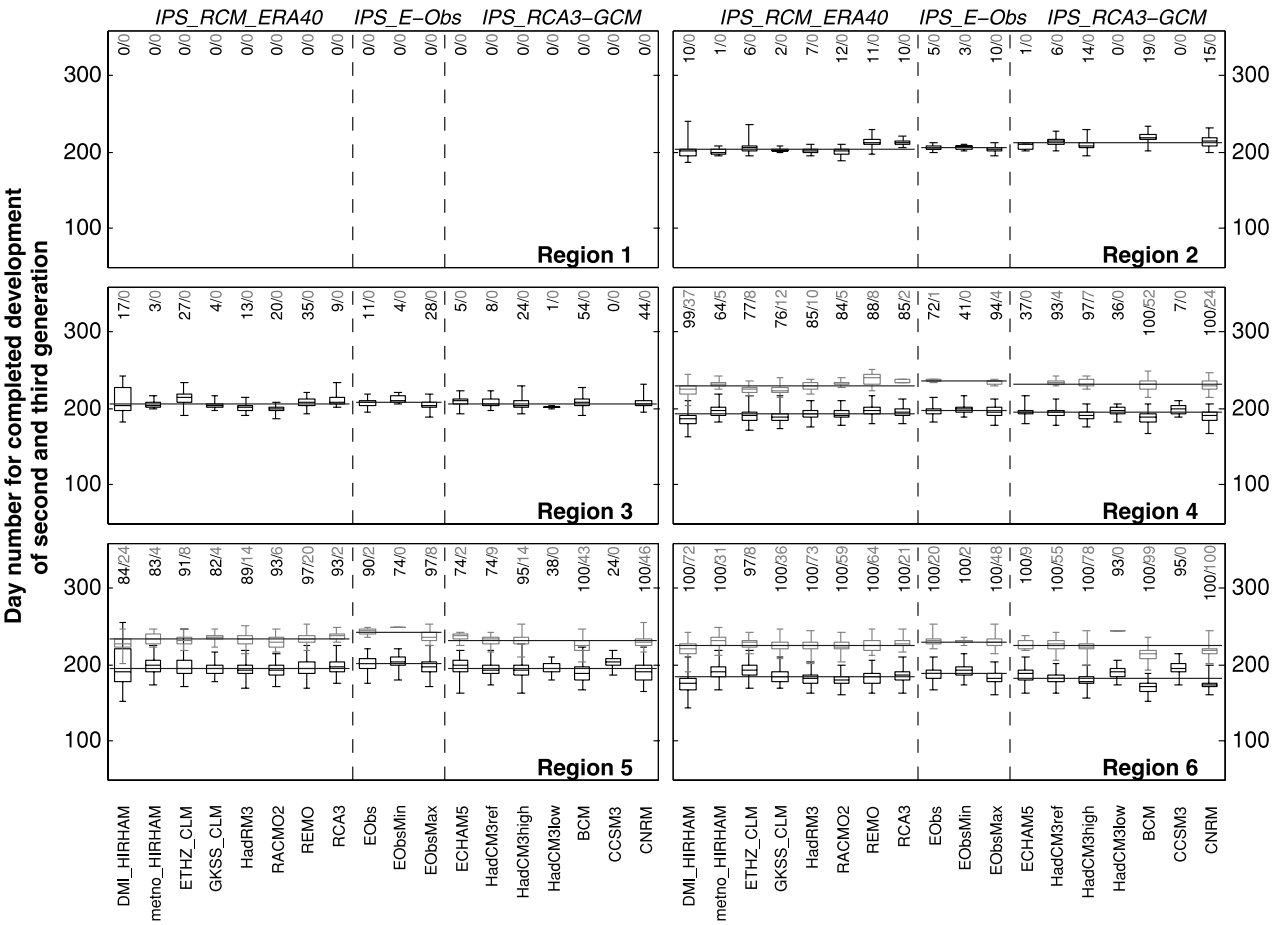

Fig. 5. Same as Fig. 4 but for initiation of a second (black boxplots) and third (grey boxplots) generation. The percent of years when a second (black numbers) and third (grey numbers) generation are initiated is indicated above the boxes.

their corresponding reference data set are shown in Table 2. In all regions, the *IPS E-Obs* best estimate and the corresponding *IPS RCM_ERA40* ensemble average differs by less than a week, except for the initiation of a third generation where the regional differences are 7–12 days. This deviation causes the *IPS RCM_ERA40* ensemble to overestimate the occurrence of a third generation. The regional mean of the *IPS RCA3_ERA40* follows the same pattern as the *IPS RCM_ERA40* ensemble average, although the mean date for initiation of a second and third generations is somewhat closer to the *IPS E-Obs* best estimate. The *IPS RCA3_GCM* ensemble means for the reference period are a few days later than the *IPS RCA3_ERA40* for regions 1–3, but a few days earlier for regions 4–6, thereby overestimating the occurrence of a third generation (Table 2).

In Fig. 6A (upper panel), the regional mean biases are illustrated by comparing the average timing of completed development of the first generation for the different ensemble members. The error bars for the individual ensemble members are narrow compared to the difference between the ensemble members, hence indicating significant differences between the *IPS RCM_ERA40* ensemble members. It is however worth noting that the combined effect of sub-gridcell variability and statistical interpolation uncertainty, represented by the *IPS E-Obs* 95% confidence interval, is much larger than the combined interannual and spatial variability within the regions (the individual error bars). In regions 4–6, most *IPS RCM_ERA40* ensemble members provide an earlier date for completed development of the first generation than the *IPS E-Obs* best estimate. Specifically, the *IPS RCA3_ERA40* underestimates the timing by 3 days. It also overestimates the timing in the north (regions 1–3) by 3–5 days. The pattern for the *IPS RCA3_GCM* reference period ensemble is somewhat different (Fig. 6B, lower panel). Here, the individual ensemble members tend have a consistent bias across the different regions Only three members change sign of bias, from a later timing in north to an earlier timing in the south.

3.2. *Future projections—trends, variability and uncertainty*

Fig. 7 provides an overview of how the regional timing of first generation maturation is projected to change in the future

Table 2. Regional summary statistics for the different IPS data sets.

IPS model phenological stage	Driving climate data set	Region					
		1	2	3	4	5	6
Initiation of first generation	E-Obs best est.	169.1 ± 0.5	152.7 ± 0.5	149.0 ± 0.5	135.5 ± 0.5	132.5 ± 0.8	119.5 ± 0.7
		100	100	100	100	100	100
	RCM_ERA40	173.9 ± 0.3	156.2 ± 0.3	150.1 ± 0.3	133.1 ± 0.2	132.1 ± 0.4	119.3 ± 0.3
		96	99	100	100	100	100
	RCA3_ERA40	174.8 ± 0.7	157.3 ± 0.5	152.5 ± 0.6	131.6 ± 0.5	130.2 ± 0.6	118.7 ± 0.5
		100	100	100	100	100	100
	RCA3_GCM	177.6 ± 0.4	161.1 ± 0.3	155.6 ± 0.3	131.8 ± 0.2	131.5 ± 0.4	116.7 ± 0.3
		78	100	99	100	100	100
Completed development of first generation	E-Obs best est.	244.5 ± 1.3	223.0 ± 0.7	220.8 ± 0.8	200.9 ± 0.5	203.2 ± 0.7	188.1 ± 0.5
		42	100	97	100	100	100
	RCM_ERA40	245.1 ± 0.7	224.2 ± 0.4	221.3 ± 0.4	195.4 ± 0.3	199.8 ± 0.4	184.4 ± 0.3
		25	95	95	100	100	100
	RCA3_ERA	249.9 ± 1.7	225.9 ± 0.7	224.1 ± 0.8	197.3 ± 0.5	199.6 ± 0.6	185.3 ± 0.5
		26	100	96	100	100	100
	RCA3_GCM	251.7 ± 1.1	231.0 ± 0.4	225.6 ± 0.5	197.2 ± 0.3	201.1 ± 0.4	183.2 ± 0.3
		12	92	90	100	100	100
Initiation of second generation	E-Obs best est.	–	205.5 ± 0.7	208.1 ± 0.8	197.0 ± 0.4	201.5 ± 0.6	188.1 ± 0.5
		0	5.3	11	72	90	100
	RCM_ERA40	–	205.7 ± 0.6	207.6 ± 0.5	192.4 ± 0.2	196.6 ± 0.3	184.3 ± 0.3
		0	7.2	16	82	89	100
	RCA3_ERA	–	212.7 ± 0.7	210.3 ± 1.1	195.2 ± 0.4	198.3 ± 0.6	185.4 ± 0.5
		0	9.8	9.1	85	93	100
	RCA3_GCM	–	214.4 ± 0.6	207.3 ± 0.3	191.8 ± 0.2	193.6 ± 0.3	182.8 ± 0.3
		0	7.9	19	67	72	98
Initiation of third generation	E-Obs best est.	–	–	–	236.6 ± 1.3	243.6 ± 1.9	232.0 ± 0.8
		0	0	0	0.6	1.9	20
	RCM_ERA40	–	–	–	227.8 ± 0.6	231.5 ± 0.6	225.1 ± 0.3
		0	0	0	11	10	45
	RCA3_ERA	–	–	–	235.6 ± 0.8	237.9 ± 2.5	228.7 ± 0.7
		0	0	0	1.9	2.2	21
	RCA3_GCM	–	–	–	231.2 ± 0.5	228.7 ± 0.5	220.1 ± 0.3
		0	0	0	12	16	49

Note: The upper line of each table entry gives the regional average and the uncertainty (S.E.) based on a 95% Student's *t* confidence interval, and the lower line gives the percentage of data that reached that development stage. *IPS E-Obs* best estimate is used as reference for the *IPS RCM_ERA40* ensemble, and *IPS RCA3_ERA40* is used as reference for the RCA3_GCM ensemble. For the *IPS RCM_ERA40* and *IPS RCA3_GCM* data sets, the table shows ensemble means across all members.

according to the different *IPS RCA3_GCM* members. The south/north gradient in timing is clearly evident in all seven *IPS RCA3_GCM* ensemble members. For regions 1–3, the high percentiles (late timing, corresponding to low temperatures) change more than the low percentiles. This suggests that the frequency distributions become less skewed. The implication of this is that the interannual variability in timing of maturation will decrease. From Fig. 7 it is also evident that there are systematic differences between the individual members. Although results from *IPS RCA3_HadCM3ref* and *IPS RCA3_HadCM3high* are similar, the low climate sensitivity version, *IPS RCA3_HadCM3low*, together with *IPS RCA3_CCSM3* consistently exhibit later

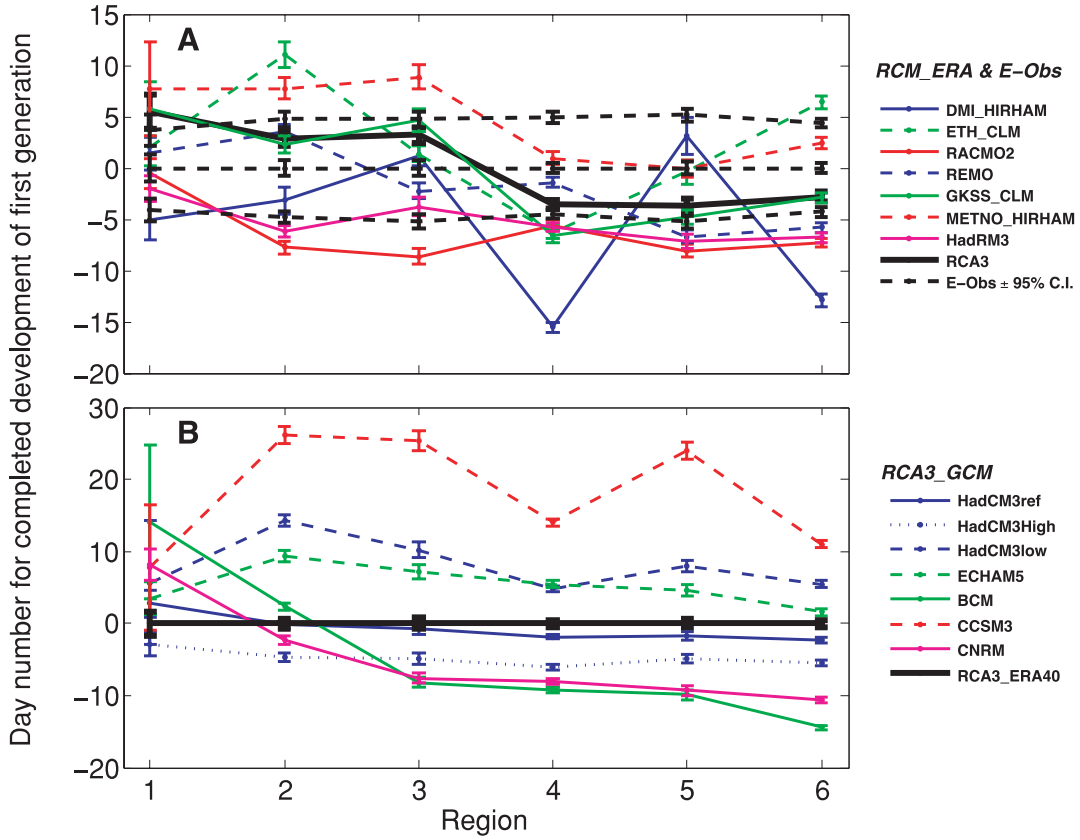

Fig. 6. Regional biases in the (A) *IPS RCM_ERA40* ensemble and (B) *IPS RCA_GCM* ensemble. Thin lines indicate each ensemble member, the thick solid line indicate the *IPS RCA3_ERA40* ensemble member, and the dashed lines indicate the *IPS E-Obs* best estimate and 95% confidence interval. For each IPS ensemble members, the regional mean and standard error was calculated across all gridcells and all years for the reference period 1961–1990. Upper panel: the *IPS RCM_ERA40* ensemble differential biases with respect to the *IPS E-Obs* best estimate (thick dashed line at $y = 0$). Lower panel: the *IPS RCA_GCM* ensemble differential biases with respect to the *IPS RCA3_ERA40* ensemble member (thick solid line at $y = 0$).

timing compared to the other ensemble members. With only few exceptions, the results suggest that the change accelerates towards the latter half of the century. Nevertheless, all ensemble members except *IPS RCA3*_HadCM3high indicate that the climate in region 1 will be to harsh even by the end of the century for completed development of one generation during all years, thereby not sustaining a persistent bark beetle population.

3.3. *Climate gradients within the distribution area of I. typographus*

Now we turn the focus from the regional to the European scale. The climate of the reference period, 1961–1990, allowed for spring flight in late April to early May in lowland parts north of the Alps, shifting to early June in mountainous regions and in the north. The second generation was initiated during June and July, and the third generation during July and August (Fig. 8A). The *IPS RCA3_GCM* ensemble mean indicate that during the period of 2011–2040 (Fig. 8B) spring flight will on average take place less than one week earlier in the entire distribution area. For the period of 2070–2097 the projected changes in timing of spring flight are larger, 10–25 days, in central Europe compared to less than 1 week in northern Europe (Fig. 8C). For the period of 1961–1990 and 2011–2040, the standard deviation of calculated spring flight timing varies between 0 and 10 days of the *IPS RCA3_GCM* ensemble members (Figs 8D and E). The standard deviation is above 10 days for the entire region for the period of 2070–2097 (Fig. 8F).

The *E-Obs* best estimate indicates a high frequency of a second generation and a lower frequency of a third generation south of 55°N for the reference period (Fig. 9A). The *IPS RCA3_GCM* ensemble average is within *IPS_E-Obs* confidence limits for the second generation, whereas the third generation exceeds the upper confidence limit by 5–20 years in south Germany (approximately region 6), parts of Poland and Lithuania (region 4) (Fig. 9B). The second and third generations are projected to become more frequent and also advance further north in response to warming (Figs 9C and D). The range in frequency estimates

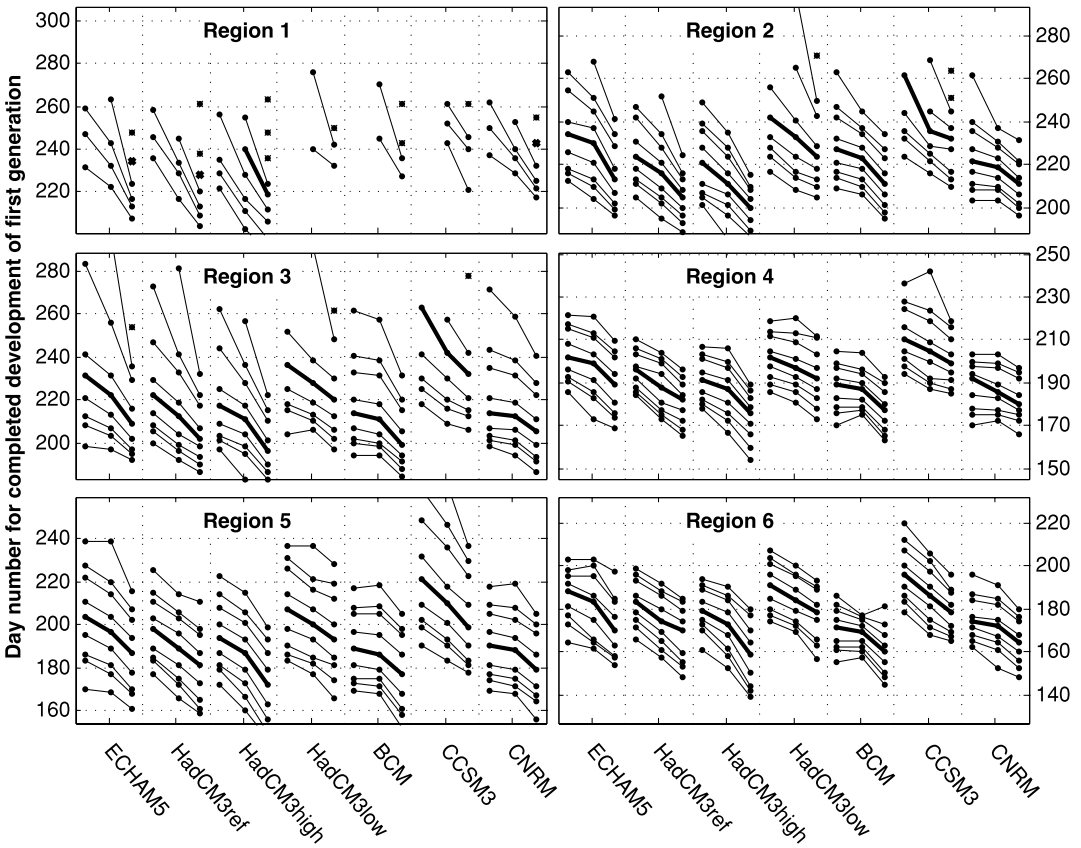

Fig. 7. Profiles showing percentiles day number for completed development of the first generation according to the *IPS RCA3_GCM* ensemble runs. The left end of each individual profile corresponds to the reference period 1961–1990, and the right end corresponds to the period 2070–2097. The 'knee in the middle' corresponds to the intermediate period 2011–2040. Each region in Fig. 3 is shown in a separate panel, having day number of completed development as y-axis and the driving GCM indicated in separate sections along the x-axis. Nine percentiles were calculated [from bottom to top: 1%, 5%, 10%, 25%, 50% (thick line), 75%, 90%, 95% and 99%] based on data for all gridcells in the region and all years in the period. If the development stage was not reached in some years the corresponding percentiles were set to missing value. In essence, in cool climatic conditions only the lowest percentiles (corresponding to the warmest years) could be calculated. If a percentile value could be calculated for one period only it is shown as a cross. Note that while the *y*-axis scale is different for each panel, the width of the interval is the same (i.e. the scale of change is constant).

between the *IPS RCA3_GCM* ensemble members is particularly high in areas undergoing a shift in dominating voltinism, that is having one to two, or two to three generations per year (Fig. 9E).

4. Discussion

In this study, we have analysed how the IPS model responds to variation and uncertainties inherent in two ensembles of regional climate simulations. We first look at how the bias pattern seen in Figs 4–6 compares to the corresponding bias pattern in the forcing climate data sets. From Kjellström et al. (2011), we extract key information regarding biases in the *RCA3_ERA40* experiment mean summer and winter temperature during the reference period 1961–1990. Compared to the *E-Obs* reference data set there is a weak negative bias (about -1 °C) in *RCA3_ERA40* summer mean temperature over the north Swedish inland and some patches north of the Alps. This bias is carried over to the IPS simulation results in region 1 (Figs 4 and 6A). Otherwise, there is no substantial bias in the *RCA3_ERA40* summer mean temperature over the study region, which is mirrored (Fig. 6A) in that the timing of the first generation maturity estimated by *IPS RCA3_ERA40* stays within the 95% confidence of the *IPS E-Obs* estimates in regions 2 to 6. In Fig. 6A, we further note that several model runs, most notably *IPS GKSS_CLM_ERA40* and *IPS REMO_ERA40* show a similar bias pattern; overestimation of the timing in the north and underestimation in the south. In Fig. 6B, the bias in the different *IPS RCA3_GCM* ensemble members are shown. Again, these biases follow to the corresponding temperature biases as presented in Kjellström et al. (2011, their Fig. 2). All in all, the median variation in Figs 4–6 follows the bias pattern of the driving climate data.

Next we turn to the influence of climatic variability on the IPS model results. The mean timing for flight of the first, second

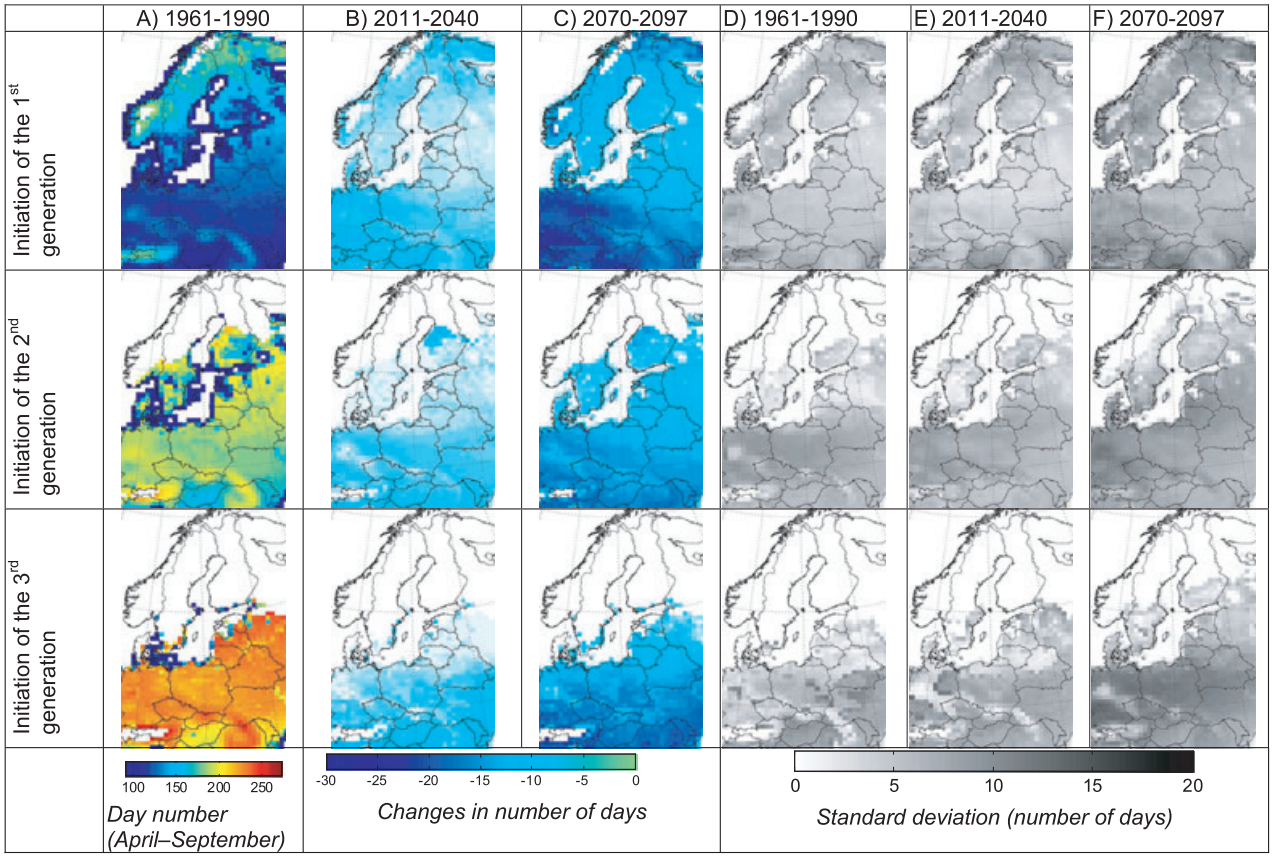

Fig. 8. (A) *IPS_RCA3_GCM* ensemble average in timing (Julian day) for initiation of the first, second and third generation during the reference period 1961–1990. Ensemble average of projected changes (number of days) in timing for (B) 2011–2040 and (C) 2070–2097, along with the ensemble standard deviation (number of days) for (D) 1961–1990, (E) 2011–2040 and (F) 2070–2097.

and third generations, as well as the corresponding frequency differed largely within the two ensemble data sets and the *IPS E-Obs* best estimate. More importantly, however, the interannual variability of the different ensembles members overlapped to a large extent (Figs 4 and 5). There are two reasons for this, the performance of the *IPS RCA3_ERA40* was relatively close to the *IPS RCM_ERA40* ensemble average in most areas and the variation in mean monthly temperature during the reference period was between 4 and 5 °C for both the *RCM_ERA40* and the *RCA3_GCM* ensemble during April to August, which is the main period of *I. typographus* activity in Europe. The variability between ensemble members was more pronounced in the *IPS RCA3_GCM* ensemble compared to the *IPS RCM_ERA40* ensemble. This is due to the variability in the different GCM's representations of the present-day large-scale circulation (Kjellström et al., 2011). It has previously been concluded that the choice of GCM in general, although no always, introduces larger uncertainty than the choice of RCM (Déqué et al., 2007; Olesen et al., 2007; Kjellström et al., 2011). For weather extremes, the choice of RCM is relatively more important compared to the GCM (Déqué et al., 2007; Kjellström et al., 2007). This has two implications in terms of the IPS modelling. First, the thresholds of $T2mean = 15$ °C and $T2max = 16$ °C are sufficiently far away from being an extreme summer temperature except for in the north of Scandinavia, for the choice of RCM to be less significant compared to the choice of GCM. And in terms of accumulated degree-days above 5 °C the additional temperature sum contributed by a presently infrequent extremely warm day does not change this conclusion. However, the warming trend will produce more extreme events in the future (Nikulin et al., 2011; Fischer and Schär, 2010) leading to a growing influence from the choice of RCM.

Focussing on the future as shown in Fig. 7, there are clear and consistent trends towards earlier maturation of the first generation in all seven ensemble members and in all (available) percentiles. The general level and spread varies between the individual members as a combined effect of GCM bias, initial conditions (i.e. natural variability) and uncertainties associated with modelling of future climate. Nevertheless, the climate change signal is obvious. The downward trend is not linear over the three periods 1961–1990, 2011–2040 and 2070–2097. In general, the trend is stronger in the latter part of this century. Also from 1961–1990 to 2011–2040 the large majority of profiles show a downward trend, with *IPS RCA3_BCM* in regions 4 and

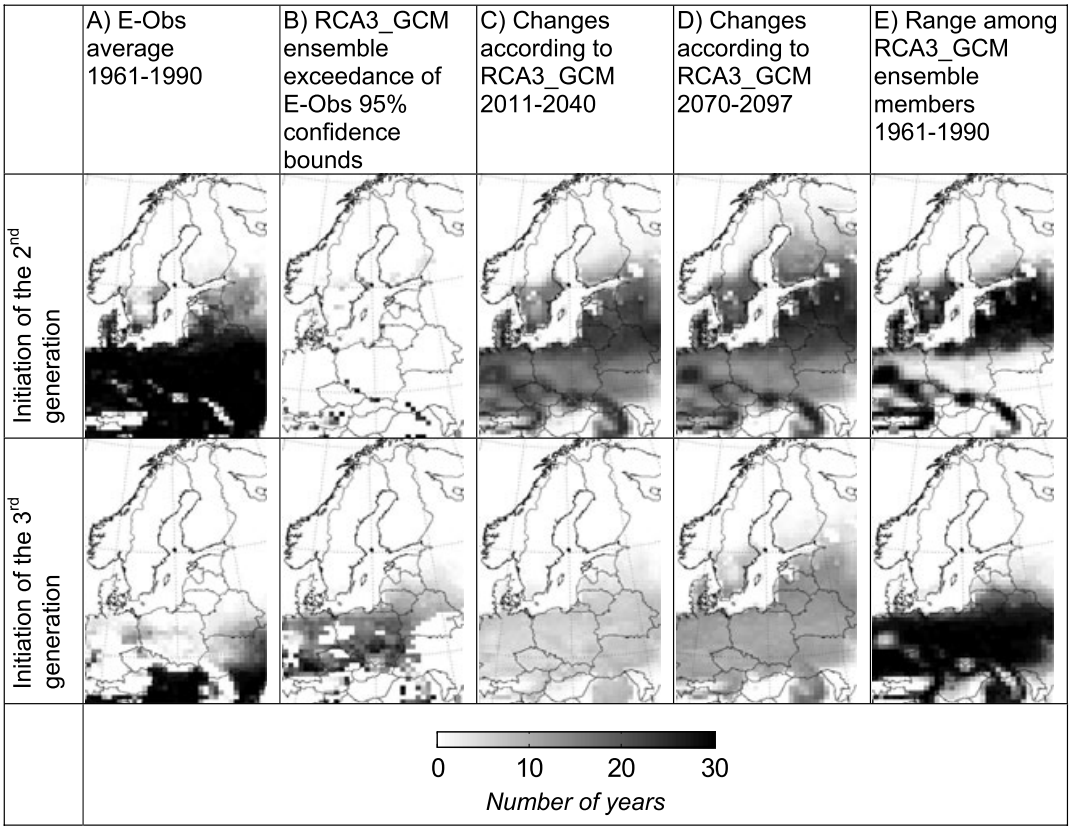

Fig. 9. (A) The number of years with initiation of a second and third generation during the reference period, 1961–1990, according to *IPS E-OBS* best estimate. (B) Deviation of the *IPS RCA3_GCM* ensemble average from the 95% confidence interval of *IPS E-Obs*. The additional number of years with initiation of a second and third generation according to the *IPS RCA3_GCM* ensemble average, calculated for the time slices of (C) 2011–2040 and (D) 2070–2097, along with (E) the range among ensemble members.

6 as the only exception of showing some consistency between the different percentile profiles. The overwhelming consistency in the downward trend between the two early periods is particularly interesting because of the relatively large influence from natural variability (initial conditions) in comparison to the climate change signal.

The IPS model is particularly sensitive to the climate data description of seasonal warming during spring (affecting the timing for crossing of the swarming temperature threshold) and seasonal cooling during autumn (affecting the timing for onset of diapause). Due to thresholds, the uncertainties within the *IPS RCA3_GCM* ensemble differs geographically from the uncertainties associated within the driving climate data set (Kjellström et al., 2011). In this study we showed that the frequency in initiation of an additional generation provides a more sensitive measure for quantifying climate variability and model uncertainty than the shift towards earlier dates. That is, the occurrence of summer flight is restricted to the time between completed development of the previous generation and onset of reproductive diapause, and the difference between climate data sets is mainly expressed by the modelled frequency of a second and third generation. The variation between IPS model runs is therefore high in regions where the interannual variations in temperature allows for one or two, respectively two or three generations. Outside these transient zones, the variation between model runs is low.

Field observations indicate that mass flight occur at daily maximum temperature above 20 °C (Annila, 1969; Wermelinger, 2004). For modelling purposes, a threshold of 16 °C has been selected to account for the differences between point measurements and grid cell averages (Jönsson et al., 2009). The flight temperature threshold of 16 °C was a reasonable approximation for the *IPS RCM_ERA40* ensemble, as the timings of initiation of the first and second generations were predominantly within *IPS E-Obs* 95% confidence intervals. It is also in accordance with the fact that the RCA3 *T2max* has a negative bias of approximately −4 °C in comparison with station observations during the bark beetle activity period (Kjellström et al., 2005). However, the simulated frequency of a third generation was outside the upper confidence limit in continental areas of central Europe. This pattern can be related to the fact that RCMs in general simulate conditions that are too warm during summer in the southeastern part of Europe, including the continental parts of central Europe (Christensen et al., 2007; Kjellström et al., 2007). These results illustrate the need for improving RCM skills (Christensen et al.,

2007) rather than a need for developing elaborated methods for correction of biases that may not hold true for extrapolation to future climate conditions. It is methodologically difficult to adjust biases that differ in magnitude between seasons and geographical regions, also accounting for natural variations between years. Related issues are whether the contribution of individual ensemble members should be weighted based on their performance, and if the criterion best suited for weighting purpose should be based on meteorological aspects or being related to the specific requirements of the impact model.

A warmer climate will lead to an earlier initiation of the first generation, accelerated development from egg to mature bark beetle, and thereby increased probability of a second (third) generation per year. There are uncertainties associated with the selected diapause model parameterization, due to lack of experimental knowledge. Without reproductive diapause, however, initiations of a second and third generations would have been more common than observed, resulting in a high frequency of incomplete development before winter. Model analyses have shown that reproductive diapause will not restrict the initiation of an additional beetle generation per year (Jönsson et al., 2010), due to earlier maturation of the first generation. The warming trend can therefore result in increased frequency of late summer swarming events, and we conclude that geographical areas undergoing a transition in dominating number of generations per year showed the largest variation in future projections among RCM3_GCM ensemble members. The large variation in the transition zones is explained by the fact that comparatively small differences in the climate can have a large impact on *I. typographus*. This implies that biological impact assessment can be sensitive to aspects and properties of climate scenario data used, and that uncertainties associated with climate modelling has to be considered. One additional concern is, however, that bark beetles developed on sites with a favourable local climate may induce an additional generation more frequently than suggested by the average gridcell climate.

5. Conclusions

1. This study indicate a shift from one to two generations of *I. typographus* per year in south Scandinavia, and an increased frequency of three generations per year in central Europe in response to a warmer climate.

2. Biological processes described by accumulation of temperature sums and responses induced after crossing of discrete temperature thresholds increase the risk for amplification of otherwise modest bias in climate data. As shown in this study, uncertainties in climate change scenarios can be particularly amplified in regions on the margin of climate change induced impact on organism performance, that is shifts in dominating voltinism of *I. typographus* caused by a temperature increase.

3. Impact assessments using an ensemble of climate change scenarios provide better support for development of adaptation and risk management strategies compared to if only one scenario is used because a scenario ensemble allows quantification of several sources of methodological uncertainties. A particular advantage is the possibility to identify regions and change signals that are robust across all, or at least a majority of the ensemble members and, likewise, to find out what is less robust. This is of particular importance in regions facing a transition in biological response.

6. Acknowledgments

This study was financially supported by the EU-FP6 project ENSEMBLES (GOCE-CT-2003–505539) and from the Swedish Mistra-SWECIA programme funded by Mistra (the Foundation for Strategic Environmental Research). Several of the RCA3 scenario simulations were done within the Nordic Climate and Energy Systems (CES) project. The RCA3 simulations were made on the climate computing resource Tornado funded with a grant from the Knut and Alice Wallenberg foundation. The groups carrying out dynamical downscaling in ENSEMBLES (http://www.ensembles-eu.org) are kindly acknowledged, as is DMI for hosting the Ensembles RCM data archive. This work greatly benefited from the ENSEMBLES *E-Obs* gridded observational climate data set hosted by the ECA&D project (http://eca.knmi.nl). We thank anonymous reviewers for constructive comments.

References

Ahti, T., Hämet-Ahti, L. and Jalas, J., 1968. Vegetation zones and their sections in northwestern Europe. *Annales Botanici Fennici* **5**, 169–211.

Anderbrant, O., 1990. Gallery construction and oviposition of the bark beetle *Ips typographus* (Coleoptera, Scolytidae) at different breeding densities. *Ecol. Entomol.* **15**, 1–8.

Annila, E., 1969. Influence of temperature upon the development and voltinism of *Ips typographus* L. (Coleoptera, Scolytiade). *Annals Zoologici Fenniciici* **6**, 161–208.

Araujo, M. B. and Rahbek, C., 2006. How does climate change affect biodiversity? *Science* **313**, 1396–1397.

Ayres, M. P. and Lombardero, M. J., 2000. Assessing the consequences of global change for forest disturbance from herbivores and pathogens. *Sci. Total Environ.* **262**, 263–286.

Bleck, R., Rooth, C., Hu, D. M. and Smith, L. T., 1992. Salinity-driven thermocline transients in a wind-forced and thermohaline-forced isopycnic coordinate model of the North-Atlantic. *J. Phys. Oceanogr.* **22**, 1486–1505.

Böhm, U., Kücken, M., Ahrens, W., Block, A., Hauffe, D. and co-authors, 2006. CLM – the climate version of LM: brief description and long-term applications. COSMO Newsletter, 6.

Buonomo, E., Jones, R., Huntingford, C. and Hannaford, J., 2007. On the robustness of changes in extreme precipitation over Europe from two high resolution climate change simulations. *Q. J. R. Meteorol. Soc.* **133**, 65–81.

Christensen, J. H., Hewitson B., Busuioc, A., Chen, A., Gao, X. and co-authors, 2007. Regional climate projections. The Physical Science

Basis. Contribution of Working Group I to the Fourth Assessment Report of the Intergovernmental Panel on Climate Change. Cambridge University Press, Cambridge, United Kingdom and New York, NY, USA, 847–940.

Christensen, J. H., Christensen, O. B., Lopez, P., van Meijgaard, E. and Botzet, M., 1996. The HIRHAM4 regional atmospheric climate model. DMI Scientific Report 96-4.

Christensen, J. H., Rummukainen, M. and Lenderink, G. (Editors), 2009. Formulation of very-high-resolution regional climate model ensembles for Europe. Met Office Hadley Centre, FitzRoy Road, Exeter EX1 3PB, UK. 160 pp.

Christiansen, E. and Bakke, A., 1988. The Spruce Bark Beetle of Eurasia. In: *Dynamics of forest insect populations* (ed. A. A. Berryman), Plenum Publishing Corporation, New York, 479–503.

Collins, W. D., Bitz, C. M. Blackmon, M. L., Bonan, G. B., Bretheron, C. S. and co-authors, 2006. The community climate system model version 3 (CCSM3), *J. Climate* **19**, 2122–2143.

Collins, M., Booth, B. B., Bhaskaran, B., Harris, G. R., Murphy, J. M. and co-authors, 2010. Climate model errors, feedbacks, and forcings: a comparison of perturbed physics and multi-model ensembles. *Clim. Dyn*., doi:10.1007/s00382-010-0808-0.

Déqué, M., Dreveton, C., Braun, A. and Cariolle, D., 1994. The Arpege/ifs atmosphere model – a contribution to the French community climate modelling. *Clim. Dyn*. **10**, 249–266.

Déqué, M., Rowell, D. P., Luthi, D., Giorgi, F., Christensen, J. H. and co-authors, 2007. An intercomparison of regional climate simulations for Europe: assessing uncertainties in model projections. *Clim. Change* **81**, 53–70.

Dolezal, P. and Sehnal, F., 2007. Effects of photoperiod and temperature on the development and diapause of the bark beetle *Ips typographus*. *J. Appl. Entomol.* **131**, 165–173.

Faccoli, M., 2002. Winter mortality in sub-corticolous populations of *Ips typographus* (Coleoptera, Scolytidae) and its parasitoids in the south-eastern Alps. *J. Pest Sci.* **75**, 62–68.

Faccoli, M., 2009. Effect of weather on *Ips typographus* (Coleoptera Curculionidae) phenology, voltinism, and associated spruce mortality in the southeastern Alps. *Environ. Entomol.* **38**, 307–316.

Fettig, C. J., Klepzig, K. D., Billings, R. F., Munson, A. S., Nebeker, T. E. and co-authors, 2007. The effectiveness of vegetation management practices for prevention and control of bark beetle infestations in coniferous forests of the western and southern United States. *Forest Ecol. Manage.* **238**, 24–53.

Fischer, E. M. and Schär, C. 2010. Consistent geographical patterns of changes in high-impact European heatwaves. *Nature Geosci*., doi:10.1038/ngeo866.

Franklin, J. F., Spies, T. A., Van Pelt, R., Carey, A. B., Thornburgh, D. A. and co-authors, 2002. Disturbances and structural development of natural forest ecosystems with silvicultural implications, using Douglas-fir forests as an example. *Forest Ecol. Manage.* **155**, 399–423.

Gordon, C., Cooper, C., Senior, C. A., Banks, H., Gregory, J. M. and co-authors, 2000. The simulation of SST, sea ice extents and ocean heat transports in a version of the Hadley Centre coupled model without flux adjustments. *Clim. Dyn.* **16**, 147–168.

Gray, D. R., 2004. The gypsy moth life stage model: landscape-wide estimates of gypsy moth establishment using a multi-generational phenology model. *Ecol. Modell.* **176**, 155–171.

Hanewinkel, M., Breidenbach, J., Neeff, T. and Kublin, E., 2008. Seventy-seven years of natural disturbances in a mountain forest area – the influence of storm, snow, and insect damage analysed with a long-term time series. *Can. J. Forest Res*. **38**, 2249–2261.

Haugen, J. E. and Haakenstad, H., 2006. Validation of HIRHAM version 2 with 50 km and 25 km resolution. RegClim General Technical Report No. 9, 159–173.

Haylock, M. R., Hofstra, N., Tank, A., Klok, E. J., Jones, P. D. and co-authors, 2008. A European daily high-resolution gridded data set of surface temperature and precipitation for 1950–2006. *J. Geophys. Res.-Atmos*. **113**, D20119, doi:10.1029/2008JD010201.

Jacob, D., 2001. A note to the simulation of the annual and inter-annual variability of the water budget over the Baltic Sea drainage basin. *Meteorol. Atmos. Phys*. **77**, 61–73.

Jacob, D., Andrae, U., Elgered, G., Fortelius, C., Graham, L. P. and co-authors, 2001. A Comprehensive Model Intercomparison Study Investigating the Water Budget during the BALTEX-PIDCAP Period. *Meteorol. Atmos. Phys*. **77**, 19–43.

Jönsson, A. M., Appelberg, G., Harding, S. and Bärring, L., 2009. Spatio-temporal impact of climate change on the activity and voltinism of the spruce bark beetle, *Ips typographus*, *Global Change Biol*. **15**, 486–499.

Jönsson, A. M., Harding, S., Bärring, L. and Ravn, H. P., 2007. Impact of climate change on the population dynamics of *Ips typographus* in southern Sweden. *Agric. Forest Meteorol*. **146**, 70–81.

Jönsson, A. M., Harding, S., Krokene, P., Lange, H., Lindelöw and co-authors, 2010. Modelling the potential impact of global warming on *Ips typographus* voltinism and reproductive diapause. *Scand. J. For. Res.* **25**, 273–274.

Jungclaus, J. H., Keenlyside, N., Botzet, M., Haak, H., Luo, J. J., and co-authors, 2006. Ocean circulation and tropical variability in the coupled model ECHAM5/MPI-OM. *J. Climate* **19**, 3952–3972.

Kjellström, E., Bärring, L., Gollvik, S., Hansson, U., Jones, C. and co-authors, 2005. A 140-year simulation of European climate with the new version of the Rossby Centre regional atmospheric climate model (RCA3). Reports Meteorology and Climatology, No 108, Dec 2005. Swedish Meteorological and Hydrological Institute, SE-60176 Norrköping, Sweden, 54 pp.

Kjellström, E., Bärring, L., Jacob, D., Jones, R., Lenderink, G. and Schär, C., 2007. Modelling daily temperature extremes: recent climate and future changes over Europe. *Clim. Change* **81**, 249–265.

Kjellström, E., Nikulin, G., Hansson, U., Strandberg, G. and Ullerstig, A., 2011. 21st century changes in the European climate: uncertainties derived from an ensemble of regional climate model simulations. *Tellus* **63A**, 24–40.

Lange, H., Økland, B. and Krokene, P. 2006. Thresholds in the life cycle of the spruce bark beetle under climate change. *Interjournal Complex Syst.* **1648**, 1–10.

Nakićenović, N. and Swart, R. (Editors), 2000. Emission Scenarios, a Special Report of Working Group III of the Intergovernmental Panel on Climate Change. Cambridge University Press, Cambridge UK, 612 pp.

Nikulin, G., Kjellström, E., Hansson, U., Strandberg, G. and Ullerstig, A., 2011. Evaluation and future future projections of temperature, precipitation and wind extremes over Europe in an ensemble of regional climate simulations. *Tellus* **63A**, 41–55.

Nilsson, C., 2008. Windstorms in Sweden – Variations and Impacts Doctoral Thesis, Lund University, Lund. Sweden, 169 pp.

Nilsson, C., Stjernquist, I., Barring, L., Schlyter, P., Jonsson, A. M. and Samuelsson, H., 2004. Recorded storm damage in Swedish forests 1901–2000. *Forest Ecol. Manage*. **199**, 165–173.

Økland, B. and Berryman, A., 2004. Resource dynamic plays a key role in regional fluctuations of the spruce bark beetles *Ips typographus*. *Agric. Forest Entomol.* **6**, 141–146.

Økland, B. and Bjørnstad, O. N., 2003. Synchrony and geographical variation of the spruce bark beetle (*Ips typographus*) during a non-epidemic period. *Populat. Ecol.* **45**, 213–219.

Økland, B. and Bjørnstad, O. N., 2006. A resource-depletion model of forest insect outbreaks. *Ecology* **87**, 283–290.

Olesen, J. E., Carter, T. R., Diaz-Ambrona, C. H., Fronzek, S., Heidmann, T. and co-authors, 2007. Uncertainties in projected impacts of climate change on European agriculture and terrestrial ecosystems based on scenarios from regional climate models. *Clim. Change* **81**, 123–143.

Oliver, C. D. and Larson, B. C., 1996. *Forest Stand Dynamics*. Wiley, New York, 544 pp.

Parmesan, C., 2006. Ecological and evolutionary responses to recent climate change. *Ann. Rev. Ecol. Evolut. Systemat.* **37**, 637–669.

Roeckner, E., Brokopf, R., Esch, M., Giorgetta, M., Hagemann, S. and co-authors, 2006. Sensitivity of simulated climate to horizontal and vertical resolution in the ECHAM5 atmosphere model. *J. Climate* **19**, 3771–3791.

Rosenzweig, C., Casassa, G., Karoly, D. J., Imeson, A., Liu, C. and co-authors, 2007. Assessment of observed changes and responses in natural and managed systems. Climate Change 2007: Impacts, Adaptation and Vulnerability. Contribution of Working Group II to the Fourth Assessment Report of the Intergovernmental Panel on Climate Change Cambridge University Press, Cambridge, UK, 79–131.

Rouault, G., Candau, J. N., Lieutier, F., Nageleisen, L. M., Martin, J. C. and co-authors, 2006. Effects of drought and heat on forest insect populations in relation to the 2003 drought in Western Europe. *Ann. Forest Sci*. **63**, 613–624.

Royer, J. F., Cariolle, D., Chauvin, F., Deque, M., Douville, H. and co-authors, 2002. Simulation of climate changes during the 21st century including stratospheric ozone. *Comptes Rendus Geoscience* **334**, 147–154.

Rummukainen, M., 2010. State-of-the-art with regional climate models. *WIREs Clim. Change* **1**, 82–96.

Samuelsson, P., Jones, C., Willén, U., Gollvik, S., Hansson, U. and co-authors, 2011. The Rossby Centre Regional Climate Model RCA3: model description and performance. *Tellus* **63A**, 4–23.

Schelhaas, M. J., Nabuurs, G. J. and Schuck, A., 2003. Natural disturbances in the European forests in the 19th and 20th centuries. *Global Change Biol*. **9**, 1620–1633.

Schroeder, L. M., 2003. Tree mortality by the bark beetle *Ips typographus* (L.) in storm-disturbed stands. *Integrated Pest Manage. Rev.* **6**, 169–175.

Seidl, R., Schelhaas, M. J., Lindner, M. and Lexer, M. J., 2009. Modelling bark beetle disturbances in a large scale forest scenario model to assess climate change impacts and evaluate adaptive management strategies. *Regional Environ. Change* **9**, 101–119.

Uppala, S. M., Kållberg, P. W., Simmons, A. J., Andrae, U., Bechtold, V. D. and co-authors, 2005. The ERA-40 re-analysis. *Q. J. R. Meteorol. Soc.* **131**, 2961–3012.

van Asch, M., Tienderen, P. H., Holleman, L. J. M. and Visser, M. E., 2007. Predicting adaptation of phenology in response to climate change, an insect herbivore example. *Global Change Biol*. **13**, 1596–1604.

Van Der Linden, P. and Mitchell, J. F. B. (eds.), 2009, ENSEMBLES: Climate Change and its Impacts: Summary of the Research and Results from the ENSEMBLES Project. Met Office Hadley Centre, FitzRoy Road, Exeter EX1 3PB, UK, 160 pp.

van Meijgaard, E., van Ulft, L. H., van de Berg, W. J., Bosveld, F. C., van den Hurk, B. J. J. M. and co-authors, 2008. The KNMI Regional Atmospheric Climate Model RACMO, Version 2.1. Available at: http://www.knmi.nl/bibliotheek/knmipubTR/TR302.pdf (Accessed 1 February 2010)

Walther, G. R., Post, E., Convey, P., Menzel, A., Parmesan, C. and co-authors, 2002. Ecological responses to recent climate change. *Nature* **416**, 389–395.

Wermelinger, B. and Seifert, M., 1998. Analysis of the temperature dependent development of the spruce bark beetle *Ips typographus* (L) (Col, Scolytidae). *J. Appl. Entomol*. **122**, 185–191.

Wermelinger, B. and Seifert, M., 1999. Temperature-dependent reproduction of the spruce bark beetle *Ips typographus*, and analysis of the potential population growth. *Ecol. Entomol.* **24**, 103–110.

Wermelinger, B., 2004. Ecology and management of the spruce bark beetle *Ips typographus* – a review of recent research. *Forest Ecol. Manage.* **202**, 67–82.